UC San Diego
UC San Diego Electronic Theses and Dissertations

Title

Glutamatergic signaling pathway drives prion induced neurodegenerative phenotype in a knock in mouse model

Permalink

Author

Khuu, Helen Kieuhan

Publication Date

2021

Peer reviewed|Thesis/dissertation

UNIVERSITY OF CALIFORNIA SAN DIEGO

Glutamatergic signaling pathway drives prion induced neurodegenerative phenotype in a knock-in mouse model

A thesis submitted in partial satisfaction of the requirements for the degree Master of Science

in

Biology

by

Helen Khuu

Committee in charge:

Professor Christina Sigurdson, Chair
Professor Gentry Patrick, Co-Chair
Professor Yimin Zou

2022

The thesis of Helen Khuu is approved, and it is acceptable in quality and form for publication on microfilm and electronically.

University of California San Diego

2022

DEDICATION

I dedicate this work to my parents and grandma. Thank you for all the encouragement and support you have given me throughout the years.

EPIGRAPH

I'm not sure why I've decided to do this. I'm not any stronger than I was, and nothing else has changed. But all the same, this time I'm not going to run away. It's okay to feel weak sometimes. It's okay to be afraid. The important thing is that we face our fears. That's what makes us strong.

Natsuki Takaya

TABLE OF CONTENTS

LIST OF FIGURES

ACKNOWLEDGEMENTS

I would like to thank my mentors Dr. Christina Sigurdson, Dr. Julia Callender, Dr. Jessica Lawrence, Dr. Patricia Aguliar and Dr. Daniel Ojeda-Juarez for their guidance and encouragement. I am extremely grateful for the support and care that they show me. Thank you for believing in my abilities as a scientist and creating an environment that allowed me to grow confident in my abilities. I would also like to thank my committee members Dr. Gentry Patrick and Dr. Yimin Zou for their expertise and feedback on my work.

I am grateful for the research assistants and undergraduate team at the Sigurdson laboratory for their assistance. Without this team, this project would not be possible.

I am thankful for my parents, family, and friends. Their support has made it possible for me to chase after my dreams.

ABSTRACT OF THE THESIS

Glutamatergic signaling pathway drives prion induced neurodegenerative phenotype in a knock-

in mouse model

by

Helen Khuu

Master of Science in Biology

University of California San Diego, 2022

Professor Christina Sigurdson, Chair
Professor Gentry Patrick, Co-Chair

Prion diseases are rapidly progressive neurodegenerative diseases characterized by

spongiform degeneration, gliosis, synaptic loss, and neuronal dystrophy. Prion disease is caused

when the cellular glycosylphosphatidylinositol (GPI)-anchored prion protein, PrP^C, misfolds into

an aggregated conformer, known as PrP^{Sc}. PrP^C has an unstructured flexible N-terminus and a

structured C-terminus with two N-linked glycans. Several human prion diseases are caused by

mutations in the N-terminus of PrP^C. For example, some cases of Gerstmann-Straüssler-

Scheinker disease or Creutzfeldt-Jakob disease are caused by insertions in the octapeptide repeat

region of the N-terminus. Furthermore, the untethered N-terminus of PrP^C can act as a neurotoxic

effector domain. Mice expressing only the N-terminus of PrP^C show altered interactions between

the truncated PrP^C and endoplasmic reticulum proteins, which results in neurotoxicity. To understand how the N-terminus impacts PrP^C function and neurodegenerative disease progression, we generated a knock-in mouse model that modifies the N-terminus of PrP^C by substituting glycine 93 to asparagine, allowing the N-terminus to be glycosylated and potentially untethered. This mutation causes spontaneous neurodegeneration without the presence of PrP^{Sc} aggregates. *In vitro* experiments support a role for excitotoxicity in the neurodegenerative phenotype of the *Prnp^{93N}* mice. Hippocampal and cortical primary neuron cultures from *Prnp^{93N}* mice display dendritic beading, which is characteristic of excitotoxic stress. The excessive dendritic beading in the *Prnp^{93N}* neurons was rescued using a glutamate receptor antagonist implicating signaling through glutamate receptors that are driving the excitotoxic insult. *In vivo* experiments also indicate a role for excitotoxicity in a brain specific region. Hippocampi of p26 *Prnp^{93N}* mice have higher phosphorylated Ca^{2+}/calmodulin-dependent protein kinase II (CaMKII) at threonine 286 (Thr286). Calcium ion binding to CaMKII activates the kinase and promotes autophosphorylation at Thr286 to constitutively activate CaMKII. Hippocampi of p26 *Prnp^{93N}* mice also show higher phosphorylated glutamate receptors, indicating increased channel conductance when compared to *Prnp^{WT}* mice. Cortex samples do not show differences. Together, this data suggests neuronal activation differs between the cortex and the hippocampus in the *Prnp^{93N}* mice. This study supports the hypothesis that enhanced excitotoxic signaling involving receptor contributes to this neurodegenerative phenotype.

Introduction

Prion disease

Prion diseases, also known as transmissible spongiform encephalopathies, are a group of fatal neurodegenerative disorders that affect both humans and animals (Sigurdson, Bartz, and Glatzel 2019). The disease is caused by the misfolding of the cellular prion protein (PrP^C) into the infectious form (PrP^{Sc}) (Westergard, Christensen, and Harris 2007). Human prion diseases are either familial (genetic mutation in the prion protein), sporadic (spontaneously occurring), or acquired (iatrogenic or transmissible) (Gaudino et al., 2017). Sporadic Creutzfeldt–Jakob disease (sCJD) is the most common human prion disease characterized by gliosis, neuronal vacuolation (spongiform change), neuronal loss, cognitive defects, motor deficits, and the accumulation of prion protein aggregates (Zerr and Parchi 2018). There are no therapies or treatments to cure prion disease; however, current studies focus on targeting PrP^C, PrP^{Sc}, or preventing PrP^C to PrP^{Sc} conversion (Chen and Dong 2021).

Many neurodegenerative diseases, such as tauopathies, have been termed "prion-like" due to similar aggregate seeding-induced protein conversion and aggregation and spread (Costanzo & Zurzolo, 2013). Furthermore, the N-terminus of PrP^C has been found to bind to amyloid beta (Aβ) oligomers, instigating a signaling cascade leading to neuronal toxicity (Zhang et al. 2019). Therefore, a better understanding of the role of PrP^C in disease pathogenesis is needed to develop effective therapies and treatments for neurodegenerative disorders.

Structure and Function of PrP^C

PrP^C is a cell surface protein with a glycosylphosphatidylinositol (GPI)-anchored tail (Stahl et al. 1992). The N-terminus (residue 23-125) is a flexible and unstructured domain, while the C-terminus (residue 126-230) is a structured domain made up of three α-helices and two

antiparallel β-strands (Donne et al. 1997; Zahn et al. 2000). The C-terminus can undergo post-translational modifications with two sites available for N-glycosylation and one for disulfide bridge formation. The N-terminus has two copper ion (Cu^{2+}) binding sites and consists of a polybasic region, an octapeptide repeat region, and a hydrophobic region (Hara and Sakaguchi 2020).

Knockout mice lacking PrP^C are resistant to PrP^{Sc} formation. In addition, mice with only one copy of PrP^C are less susceptible to PrP^{Sc} infection (Bueler et al. 1993). However, these knockout mice show abnormal circadian rhythms, impaired neuronal excitability, increased susceptibility to excitotoxic insult, and N-terminal PrP^C-mediated toxicity (Steele, Lindquist, and Aguzzi 2007). PrP^C functions are not entirely known, but one proposed function suggests regulating glutamate receptor activity to protect against excitotoxic insult (Wulf, Senatore, and Aguzzi 2017). It is of interest to understand how PrP^C interacts with its cofactors to modulate function, and how these functions are deregulated during pathogenesis.

<u>The role of PrP^C in mediating neurotoxicity</u>

PrP^C has been linked to toxic signaling pathways implicated in neurodegenerative phenotypes. Previous studies have shown that genetically deleting PrP^C in prion-infected mice will reverse brain pathology and disease progression in the mice, suggesting that PrP^C is the culprit for prion disease pathology (Mallucci et al., 2003). Other studies support the hypothesis that PrP^C, not PrP^{Sc}, mediates toxic signaling, causing neurodegeneration during prion infection. Brain grafts from mice expressing PrP^C were transplanted into PrP^C knockout mice. After prion infection, it was found that only the brain graft region showed pathology despite there being PrP^{Sc} present in PrP^C knockout areas, suggesting endogenous expression of PrP^C is needed for neuronal toxicity (Brandner et al. 1996).

Past research has provided evidence that the N-terminus of PrP^C mediates toxic signaling (Wu et al., 2017). Studies in mice expressing only the N-terminal domain of PrP^C reveal that this truncated PrP^C has an altered interaction with endoplasmic reticulum proteins and causes a neurodegenerative phenotype (Dametto et al. 2015). Furthermore, mice lacking PrP^C residues 105-125 experience neurodegeneration without PrP^{Sc} aggregates. This phenotype is rescued in a dose-dependent manner by wild type (WT) PrP^C expression, suggesting that WT PrP^C and the shortened PrP^C compete to bind a target that regulates neurodegenerative signaling (Li et al. 2007). One PrP^C ligand of interest is the N-methyl-D-aspartic acid receptor (NMDAR), which has been shown to play a central role in excitotoxic signaling in many neurodegenerative diseases.

<u>PrP^C moderating excitotoxicity in neurodegenerative disease</u>

Excitotoxicity is cell death caused by prolonged activation of glutamate receptors such as NMDAR. Specifically, signaling through extrasynaptic NMDA receptors promotes cell death while synaptic NMDA receptor signaling promotes cell survival (Parsons and Raymond 2014). PrP^C knock out mice are found to have more NMDAR activity than WT mice and are more sensitive to excitotoxic insult, suggesting that PrP^C has a role in mediating NMDAR hyperactivity (Black et al. 2014). Neurons from mice with deletions in the N-terminus of PrP^C show enhanced susceptibility to glutamate mediated excitotoxicity, and this effect is restored when the neurons are treated with an NMDAR antagonist (Biasini et al. 2013). These studies support a role for PrP^C regulating NMDA receptor activity and contributing to excitotoxic cell death during neurodegeneration. PrP^{Sc} binds to PrP^C and attenuates its usual interactions with NMDAR to induce toxic signaling leading to neuronal death. Amyloid-beta oligomers have also been shown to bind to the N-terminus of PrP^C to initiate this same signaling pathway and leading

to neurotoxic death in Alzheimer's disease (Biasini et al., 2012). Thus, a model is needed to understand the interaction between PrP^C and NMDA receptors during disease progression.

<u>A knock in mouse model to study excitotoxic signaling</u>

Based on these results, more studies on blocking this toxic signaling from PrP^C are needed to develop prion disease treatments. To understand how the N-terminus of PrP^C impacts neurodegeneration, we used knockin mice that express an extra glycan. These mice have a glycine 93 to asparagine point mutation (human numbering) allowing the N-terminus to be glycosylated. These mice experience spontaneous neurodegeneration without the presence of PrP^{Sc} aggregates. Characterization of these mice has shown that the *Prnp^{93N}* homozygous (*PrnP$^{93N/93N}$*) die at around postnatal day 25-30 (p25-p30) and do not show any behavioral developmental defects. Primary neurons from *Prnp$^{93N/93N\ mice}$* display excessive dendritic varicosity, a hallmark of excitotoxic stress, and this varicosity is rescued when treated with NMDA antagonist, MK801 (dizocilpine maleate, (+)-5-methyl-10,11-dihydro-5H-dibenzo[a,d]cyclohepten-5,10-imine maleateor). Biochemical analysis of the *Prnp$^{93N/93N}$* brains shows region-specific sensitivity to excitotoxicity. These results provide evidence that the altered PrP^C enhances the excitotoxic signaling that contributes to the neurodegenerative phenotype.

Methods

<u>Animals</u>

All mice are housed in a 12-hour light/ dark cycle and have access to food and water to their liking. All mice handling complies with the University of California, San Diego's Institutional Animal Care and Use Committee standards.

<u>Behavioral Tests</u>

All behavior assays performed tested sensorimotor and vestibular development at p7, p8, p9, p10. Experimenters were blinded to the genotype of the mice at the time of testing. The assays were performed on male and female mice across three litters with 6 *Prnp*$^{93N/93N}$ and 5 *Prnp*^{WT} used for analysis.

    I.   *Sensorimotor and vestibular testing*

    a.   Negative Geotaxis

Pups were placed on a 45-degree slope with their heads facing down the slope. The time it took for the mouse to turn 180- degrees with its head facing upward was recorded with a maximum latency of 3 minutes.

    b.   Cliff Aversion

Pups forepaws were placed on the edge of a 5-inch-tall cardboard box. The time it took for the mice to retract and turn away from the edge was recorded with a maximum latency of 3 minutes.

Body Weight

Both males and females across three litters were weighed (grams) daily starting from p5 to p25. Experimenters were blinded to the genotype of the mice at the time of weighing.

Brain Tissue Collection, Homogenization, and Lysis

Cortex samples from p20 and p26 mice were collected and snap-frozen with liquid nitrogen. Cortex samples of p20 mice were homogenized in 4% sarkosyl in PBS with protease inhibitors and phospho-stop in a bead beater tissue homogenizer to create a 10% brain homogenate. Samples were then lysed with 4% sarkosyl and benzonase on ice for 30 minutes, vortexing every five minutes. Cortex samples of p26 mice were homogenized in RIPA buffer (50mM Tris-HCl pH 7.4, 150mM NaCl, 1mM EDTA, 1% NP40, 0.5% DOC, 0.1% SDS) with protease inhibitors

and phospho-stop in a bead beater tissue homogenizer to create a 10% brain homogenate. Samples were then lysed with RIPA buffer at 4-degrees with rotation for 30 minutes.

Western Blot Analysis

Equal protein levels were quantified using a BCA (bicinchoninic acid protein assay). Brain samples at p20 were loaded on a 4-12% Bis-Tris gel with MOPS running buffer and transferred to a nitrocellulose membrane by wet blotting. Brain samples at p26 were loaded on a 10% Bis-Tris gel with MES running buffer and transferred to a nitrocellulose membrane by wet blotting. Membranes were blotted overnight at 4-degrees in primary antibodies, Rab5 (Cell Signaling Technology (CST), Cat #: 3547), Rab7 (CST, Cat #: 9367), Hrs (CST, Cat #: 15087), CaMKII (Ca^{2+}/calmodulin-dependent protein kinase II) (CST Cat #: 4436), Phospho-CAMKII (Thr286) (CST, Cat #: 12716), Glun2B (NMDA receptor subtype 2B) (CST Cat #: 14544), Phospho-Glun2B ((Ser1303) (Millipore Sigma, Cat #: 07-398), and Glyceraldehyde 3-phosphate dehydrogenase (GAPDH) (Novus Biologicals Cat #: NB300-324) in either 1X casein blocking buffer or 1% BSA (bovine serum albumin) followed by one hour incubation in HRP-conjugated IgG secondary antibody at room temperature. Membranes were then imaged using a chemiluminescent substrate and visualized on a Fuji LAS 4000 imager. Images were quantified using the software Multi Gauge version 3.0.

Primary Neuron Cell Culture

Primary cortical neurons were extracted from p0 *Prnp^{93N}* mice and maintained in neuron culture media (Neurobasal plus, 1% glutamax, 2% B27 plus, and 5% Pen-Strep). Cortexes were dissected from mice in dissection media (EBSS, 6mM MgC2L, 0.25mM CaCL2, 0.9% glucose, and 10mM HEPES) then dissociated by trypsin for 15 minutes at 37-degrees. After trypsinization, DNAse was added, and cells were titrated and strained through a 100uM strainer.

Cells were spun down then resuspended in high glucose media (neuron culture media and 2.77M glucose) to remove additional debris. Cells were then spun down and then resuspended in culture media. Cells were then plated on PLL coated coverslips for imaging experiments.

Drug treatment of the primary neurons

Neurons were treated with MK801 or a water vehicle at (DIV) 21 for 72 hours. MK801 and water were delivered to the neurons in a half media change. The final concentration of MK801 used was 10uM per coverslip, and the vehicle coverslips got the same final concentration of water as the drug treated wells.

Immunofluorescent Staining of Primary Neuron Cultures

When neurons were days in vitro (DIV) 21-28, neurons were washed in 1X PBS and fixed in 4% paraformaldehyde for 15 minutes at room temperature. Neurons were permeabilized with PHEM-T (60mM PIPES pH6.9, 25mM HEPES, 10mMEGTA, 2mM MgCL2X6H2O, 0.5% Triton X-100) for 5 minutes at room temperature. Neurons were then washed with PHEM-Wash (60mM PIPES pH6.9, 25mM HEPES, 10mMEGTA, 2mM MgCL2X6H2O, 0.1% Triton X-100) and incubated in primary antibody MAP2 (Microtubule-associated protein 2) (mouse) (Millipore, Cat# MAB378; 1:1000) diluted in AbDil buffer (150mM NaCl, 20mM Tris-HCl pH 7.4, 0.1% Triton X-100, 2% BSA, 0.1% NaN3) at 4-degrees overnight followed by incubation with secondary antibody diluted in AbDil for 1 hour at room temperature. Neurons were then washed and incubated with DAPI to mark nuclei. Coverslips were then mounted onto slides using pro-long gold mounting media. A 10X objective on the fluorescent Olympus IX81 was used to view hippocampal neurons, and images were taken with the Hamamatsu ORCA-ER camera by the SlideBook 5.5 software. Images for the primary cortical neurons were taken by the same camera,

software, and microscope with a 20X objective. ImageJ2 was used to analyze neurons for percent

dendrite beading per neuron (Rueden et al. 2017).

Immunofluorescent Staining of Brain tissue samples

Paraffin embedded brain tissue from 5 p20-p22 $Prnp^{93N/93N}$, 5 p20-p22 $Prnp^{WT}$, 5 p25-p27

$Prnp^{93N/93N}$, and 4 p25-p27 $Prnp^{WT}$ were stained with dendritic and soma marker MAP2. For

immunolabeling, sections were deparaffinized, heated in citrate buffer (Sigma, Cat# C9999-

1000) with 0.05% Tween20 in a pressure cooker for 30 minutes, quenched in 3% H_2O_2 in

methanol for 15 minutes, and blocked in TNB buffer [0.5% TSA Blocking Reagent

(PerkinElmer, Cat# FP1020) in 100 mM Tris-HCl buffer (pH 7.5) with 150 mM NaCl]

containing 5% goat serum (Sigma, Cat# G9023). All primary and secondary antibodies were

diluted in TNB buffer with 5% goat serum. Slides were then incubated in the primary antibodies,

MAP2 (mouse) (Millipore, Cat# MAB378; 1:200) overnight at 4 degrees Celsius. Arc was

visualized using the goat anti-rabbit IgG Cy3 secondary antibody (Jackson ImmunoResearch,

Cat# 111-165-144) (1 hour). The MAP2 antibody was visualized using biotin goat-anti-mouse

(Jackson ImmunoResearch, Cat# 115-066-072) (30 minutes), then streptavidin-HRP (Jackson

ImmunoResearch, Cat# 016-030-084) (30 minutes), followed by tyramide Alexa 488

(Invitrogen, B40953). All slides were incubated in DAPI and mounted using ProLong Gold

(Thermo Fisher). Cells were visualized and taken with the 20X objective described in

immunofluorescent staining of primary neuron cultures.

Statistical analysis

A Student's t-test (two-tailed, unpaired) was used to analyze the $Prnp^{93N/93N}$ and $Prnp^{WT}$ mice for

the protein levels of Hrs, Rab5, Rab7, LC3B-II/I, p62, pGluN2B, pCaMKII, Glun2B, and

CaMKII. A one-way ANOVA with Tukey's post-test was used to assess the percent beaded per

neuron in the $Prnp^{93N/93N}$, $Prnp^{93N/WT}$, and $Prnp^{WT}$ mice. A Two-way ANOVA with no post-test was used to analyze the weights of the mice. Behavioral assays were analyzed using a two-way ANOVA with genotype and age as the two factors. A Bonferroni post hoc test was used for multiple comparisons to analyze the $Prnp^{93N/93N}$, $Prnp^{93N/WT}$, and $Prnp^{WT}$ mice. Statistical analysis was done on GraphPad Prism 5 software for western blot and primary neuron quantification. GraphPad Prism 8 software was used to analyze mouse behavior study and weights. A $p \leq 0.05$ was considered statistical significance, and data represent mean $\pm$ SEM.

Results

The $Prnp^{93N/93N}$ mice exhibit differences in weight gain by terminal disease

The $Prnp^{93N/93N}$ mice develop terminal disease at p28-p34 and experience clinical signs such as kyphosis and "tiptoe walk" starting at p18-20. To better understand when phenotypic differences might appear, mice were weighed from p5 to p25. From p5 to p21, the $Prnp^{93N/93N}$, $Prnp^{93N/WT}$, and $Prnp^{WT}$ littermates show no differences in weight (Fig. 1). At p22, the $Prnp^{93N/93N}$ weigh significantly less than the $Prnp^{93N/WT}$ and $Prnp^{WT}$ littermates (Fig. 1). The differences in weight observed in the $Prnp^{93N/93N}$ mice coincides with the onset of clinical signs.
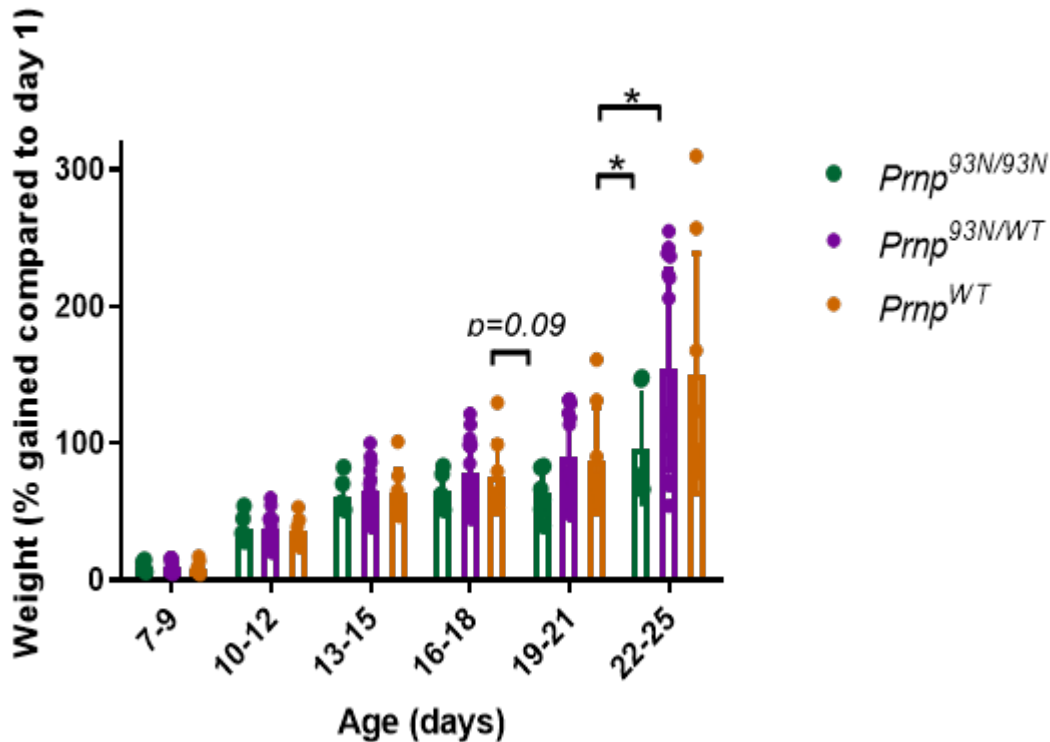
Figure 1. The *Prnp^{93N/93N}* mice do not gain as much weight as *Prnp^{WT}* and *Prnp^{93N/WT}* littermates starting at p19. Daily weight measurements show that beginning at p19, the *Prnp^{93N/93N}* mice gain less weight than their littermates and reach significant differences starting at p22. Across three litters, there are a total of n=6 *Prnp^{93N/93N}*, n=16 *Prnp^{93N/WT}* mice, and n=5 *Prnp^{WT}* mice. Statistical analysis was calculated using Two-way ANOVA with a Bonferroni post hoc test. *$p < 0.05$, **$p < 0.01$.
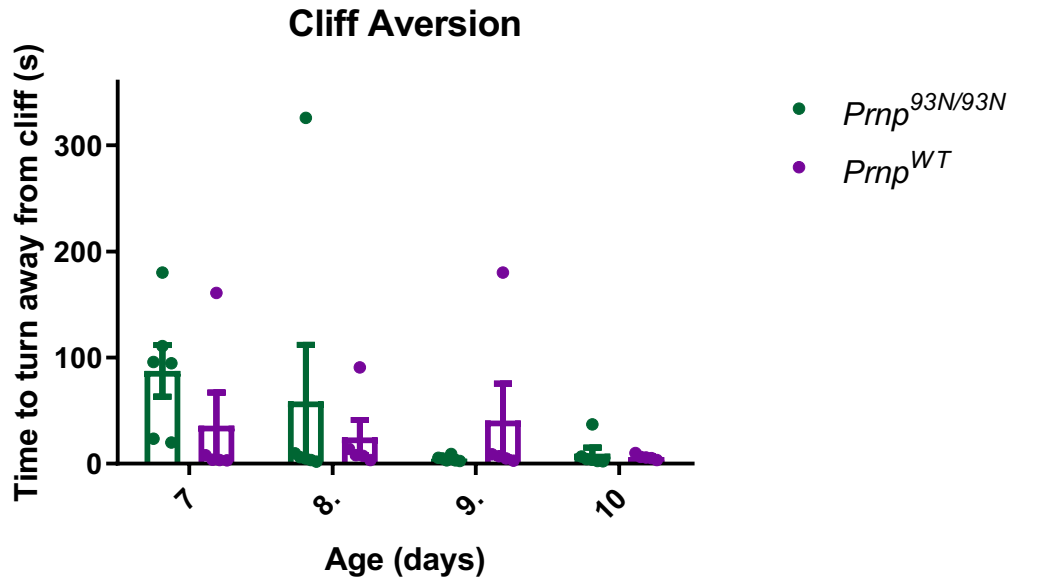
The *Prnp^{93N/93N}* mice display no developmental deficits in their sensorimotor reflexes

To assess for developmental differences between *Prnp^{93N/93N}* mice and *Prnp^{WT}* mice, pups were

subjected to negative geotaxis and cliff aversion behavioral tests. The negative geotaxis assay

assesses the proprioceptive sense and vestibular function, as mice use their sensory cues and

motor coordination to move against gravity and position their heads up an inclined slope

(Ruhela, 2019). *Prnp^{93N/93N}* mice and *Prnp^{WT}* mice at p7, p8, p9, p10, and p11 were tested.

Prnp^{93N/93N} mice show no deficits in negative geotaxis compared to WT littermates (Fig. 2A).

The cliff aversion assay evaluates sensory development and the vestibular system as mice placed

on a cliff retract from the edge (Feather-Schussler, 2016). The *Prnp^{93N/93N}* mice show no

differences in latency in the cliff aversion test compared to the *Prnp^{WT}* mice (Fig. 2B). Both the

negative geotaxis and cliff aversion assays suggest that there are no differences in sensory and

vestibular development in the mice.

Cliff Aversion

a)
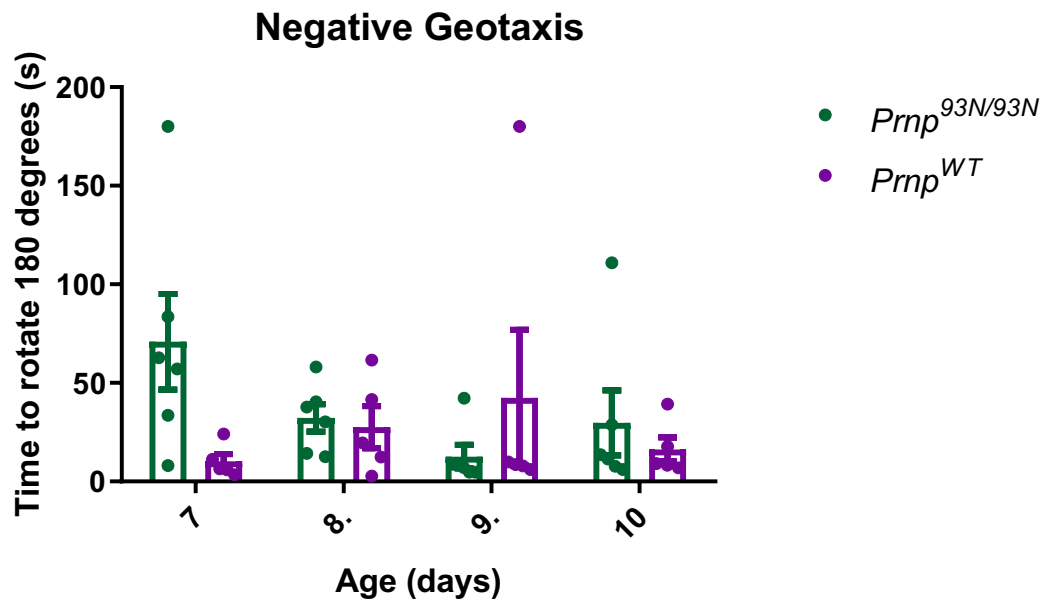
Negative Geotaxis

b)

Figure 2. The *Prnp^93N/93N* mice do not have phenotypic differences in sensorimotor and vestibular system development. Testing (a) the negative geotaxis assay and (b) the cliff aversion assay across three litters of mice at p7, p8, p9, and p10 with 6 *Prnp^93N/93N* mice and a total of 5 *Prnp^WT* mice. Statistical analysis was calculated using two-way ANOVA with a Bonferroni post hoc test.

The *Prnp⁹³ᴺ/⁹³ᴺ* mice exhibit dendritic damage in brain tissue sections

To assess dendrites in the $Prnp^{93N/93N}$ mice, paraffin embedded brain tissues were stained for MAP2 at p20 and p26. Three of the five brain tissue samples from p20 $Prnp^{93N/93N}$ show dendritic and soma loss in the CA1 region of the hippocampus (Fig. 3A). This suggests that loss of the CA1 region of the hippocampus happens during or before the first onset of clinical signs. Three of the five brain tissue samples of p26 $Prnp^{93N/93N}$ mice show loss of dendrites and loss of somas in the CA1 region of the hippocampus (Fig. 3B). This suggests that dendritic and neuronal loss to the hippocampus continues during disease progression.
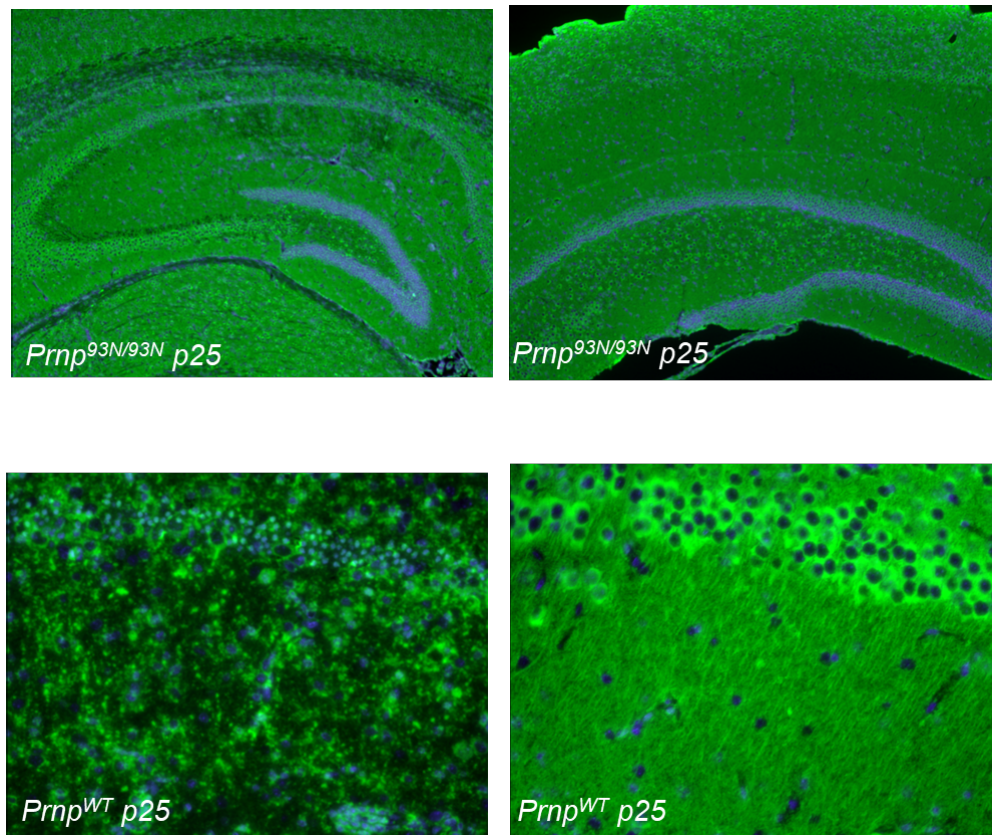

Figure 3. The *Prnp⁹³ᴺ/⁹³ᴺ* mice show signs of dendritic and soma damage at p25. $Prnp^{93N/93N}$ show signs of soma and dendritic loss in the CA1 region of the hippocampus when compared to $Prnp^{WT}$. This difference appears more pronounced at p25-p27.

<u>Primary *Prnp*$^{93N/93N}$ neurons exhibit excessive dendritic beading due to excitotoxicity</u>

Hippocampal (Fig. 4a) and cortical (Fig. 5a) neuron cultures were stained with the dendrite and

soma marker MAP2. Hippocampal and cortical neuron experiments reveal that the *Prnp*$^{93N/93N}$

mice show the most dendritic beading, and the *Prnp*^{WT} mice show the least beaded morphology.

The hippocampal *Prnp*$^{93N/WT}$ mice exhibit a significant increase in beading phenotype when

compared to the *Prnp*^{WT} mice and considerably less than the *Prnp*$^{93N/93N}$ mice, indicating that the

presence of a WT allele is enough to partially rescue the phenotype. Dendritic beading has been

associated with excitotoxicity in NMDA-treated hippocampal slices (Hoskison, 2007). Other

studies have shown that applying exogenous glutamate to cultured neurons causes dendritic

beading *in vitro* (Mizielinska et al., 2009). To determine if the beading phenotype observed in

the *Prnp*$^{93N/93N}$ is associated with excitotoxic signaling through the NMDA receptor, cortical

neurons were treated with the noncompetitive NMDA antagonist, MK801. The beading

phenotype in the *Prnp*$^{93N/93N}$ mice and *Prnp*$^{93N/WT}$ mice is rescued when cortical cultures are

treated with MK801 (Fig. 5b). This rescue suggests that stimulation of the NMDA receptor is a

factor in causing excitotoxicity in the *Prnp*^{93N} neurons.
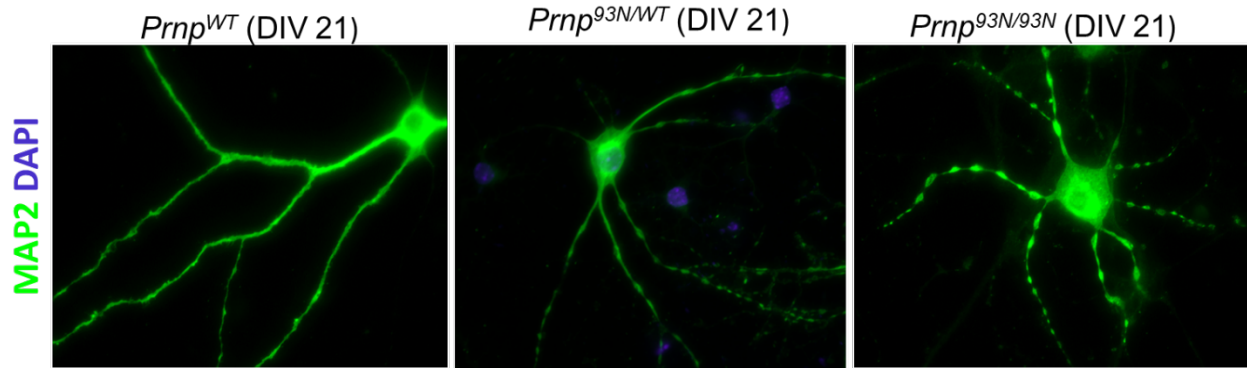
a)
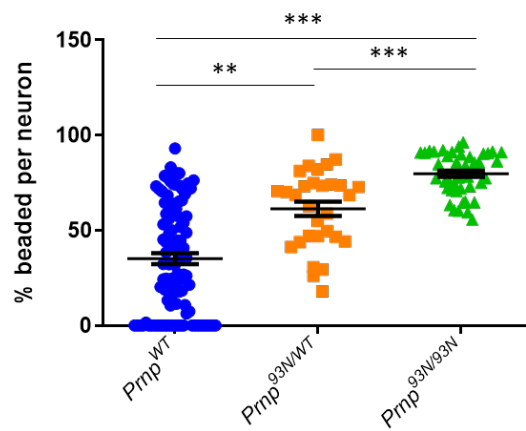
b)

Figure 4. Primary neurons from *Prnp*$^{93N/93N}$ show increased dendritic beading. Across four neuronal culture, 3 *Prnp*$^{93N/93N}$, 4 *Prnp*^{WT}, and 3 *Prnp*$^{93N/WT}$ neurons were stained with MAP2 (a). The neurons of the *Prnp*$^{93N/93N}$ show the most dendritic beading and the *Prnp*$^{93N/WT}$ show the least amount of beading (b). Statistical analysis was calculated using a one-way ANOVA with Tukey's post hoc test. *p<0.05, **p<0.01, ***p<0.001.
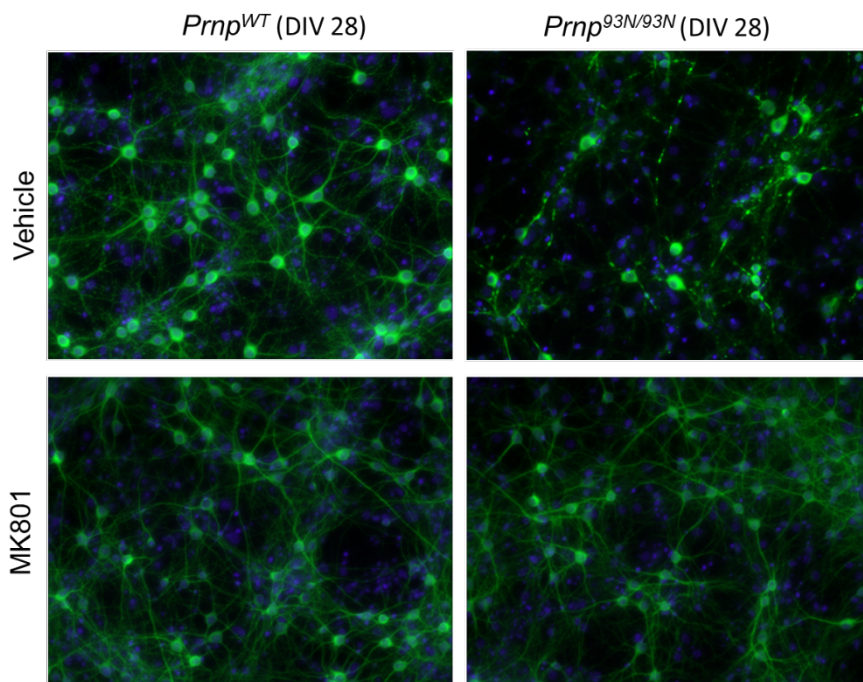
a)
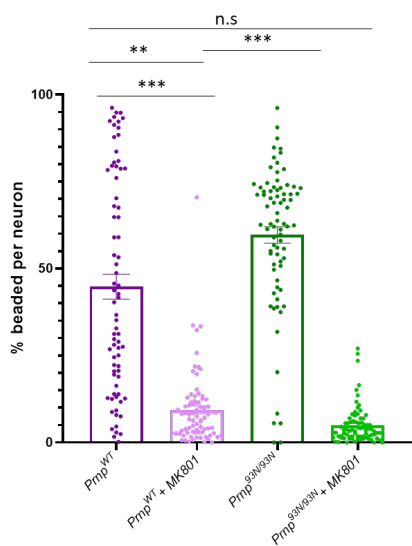
b)

Figure 5. The excessive beading from the primary neurons of *Prnp$^{93N/93N}$* treated with MK801 is rescued. In one neuronal culture, 1 *Prnp$^{93N/93N}$* and 1 *Prnp^{WT}* were treated with 10uM MK801 or vehicle and stained with MAP2 (a). The significant difference in dendritic beading between the *Prnp$^{93N/93N}$* neurons and the *Prnp$^{93N/WT}$* is gone when neurons are treated with MK801 (b). Statistical analysis was calculated using a one-way ANOVA with Tukey's post hoc test. *p<0.05, **p<0.01, ***p<0.001, n.s.= not significant.

The *Prnp[93N/93N]* cerebral cortex show no alterations in proteins involved in glutamate-mediated excitotoxicity

Previous data in the laboratory has shown that hippocampal samples from *Prnp[93N/93N]* mice display higher levels of phosphorylated-CAMKII at Thr 286 and phosphorylated-Glun2B at Ser1303, suggesting higher calcium influx and higher NMDAR channel conductance, consistent with excitotoxicity as a mechanism for neuronal death. To investigate if these findings in the hippocampus also apply to the cortex, p26 cerebral cortex samples were immunoblotted for phosphorylated-CAMKII at Thr 286 and phosphorylated-Glun2B at Ser1303 (Fig. 6). The *Prnp[93N/93N]* cortices showed no differences in these protein levels compared to *Prnp[WT]* cortices. This suggests that the cerebral cortex is less sensitive to excitotoxic insult in this context.
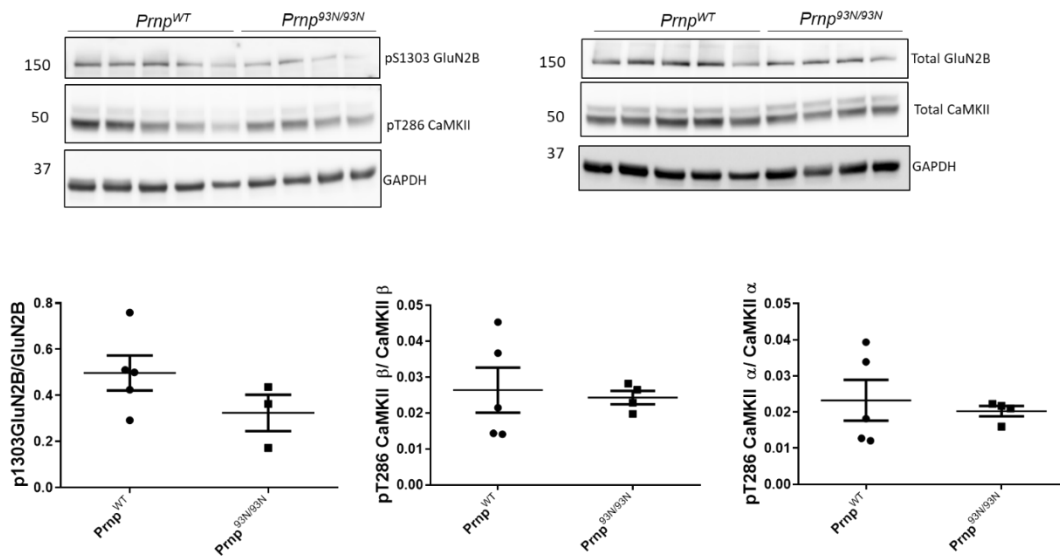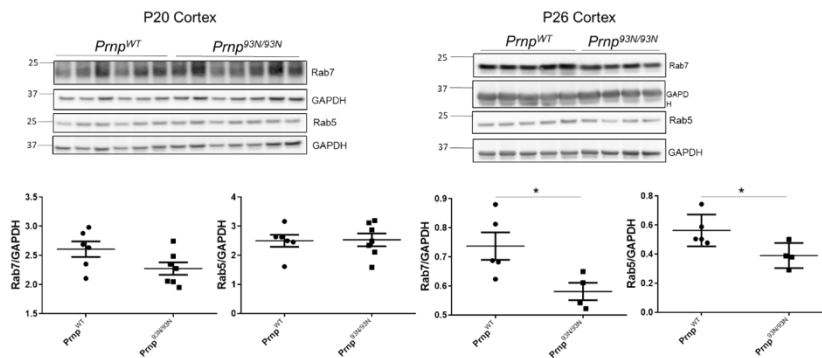

Figure 6. The *Prnp[93N/93N]* cortices show no differences in proteins associated with excitotoxic signaling. The cortices of 4 p26 *Prnp[93N/93N]* mice show similar protein levels of phosphorylated T286 CaMKII, phosphorylated S1303 GluN2B, CaMKII, and GluN2B when compared to the cortices of 5 p26 *Prnp[WT]* mice. Statistical analysis was calculated using a Student's t-test with Tukeys post hoc test.

The *Prnp[93N/93N]* mice show downregulation of endolysosomal proteins at a later stage of disease

Proper receptor degradation or recycling depends on appropriate crosstalk between the endocytic pathway and the autophagosome pathway (Wang et al. 2018). We reasoned that the

endolysosomal pathway would be affected in the *Prnp^{93N/93N}* mice. Cortices of pups at p20 (at the start of the clinical phase) and p26 (when clinical signs are severe) were immunoblotted (Fig 7.). At p20, Hrs, Rab7, and Rab5 protein levels were not significantly different between the *Prnp^{93N/93N}* and *Prnp^{WT}* mice. However, at p26, Hrs, Rab7, and Rab5 protein levels were lower in the *Prnp^{93N/93N}* mice compared to the *Prnp^{WT}* mice. These data suggest that downregulation of the endolysosomal pathway or cell loss between p20 and p26, after the first appearance of clinical signs.

a)
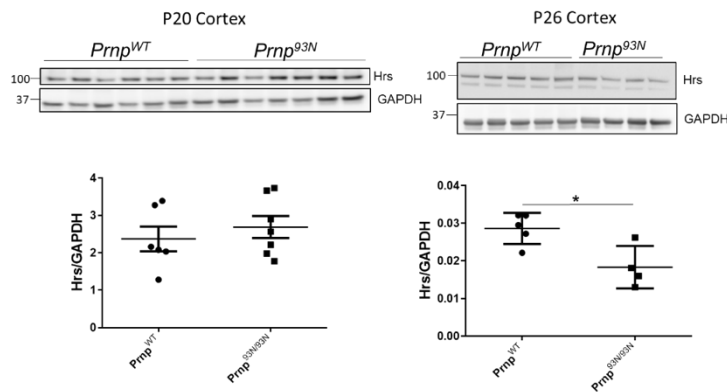
b)

Figure 7. The *Prnp^{93N/93N}* cortices show lower levels of endolysosomal proteins at late stage disease. At p20, the *Prnp^{93N/93N}* corticies show no differences in protein levels of Hrs, Rab5, and Rab7. At p26 *Prnp^{93N/93N}* cortices show lower protein levels of Hrs, Rab5, and Rab7. Statistical analysis was calculated using a Student's t-test with Tukeys post hoc test. *p<0.05.

Discussion

The function of PrP^C is still unclear, yet recent evidence suggests that it is involved in glutamate receptor signaling and is linked to excitotoxicity (Wulf, Senatore, and Aguzzi 2017). In this study, a new knock-in mouse model that expresses tri-glycosylated PrP^C was used to understand the role of PrP^C in NMDAR-mediated excitotoxicity. The *Prnp$^{93N/93N}$* mice develop severe neurodegenerative disease. They experience clinical signs at p18-20 and are terminal at p28-p34. Starting at p22, the *Prnp$^{93N/93N}$* mice gain less weight than the WT mice. The mice also do not exhibit detectable differences in vestibular and sensory development.

In vivo experiments implicate NMDAR mediated excitotoxicity as a driver of the neurodegenerative phenotype of the *Prnp$^{93N/93N}$* mice. Excitotoxicity is defined as cell death caused by toxic agents from the overactivation of excitatory receptors (Dong, Wang, and Qin 2009). Historically, dendritic beading is a hallmark of neuronal toxicity *in vitro* (Greenwood and Connolly 2007). Hippocampal and cortical neurons from the *Prnp$^{93N/93N}$* mice show more dendritic beading per neuron than the *Prnp^{WT}* mice. This difference in the percentage of beading per neuron was ablated when the cultures were treated with the noncompetitive NMDAR antagonist, MK-801. MK-801 binds to the NMDA receptor at the transmembrane domain (TMD), decreasing Ca^{2+} influx and blocking the overactivation of the NMDA receptor that could lead to the release of toxins that causes apoptosis and necrosis (Lipton 2004; Song et al. 2018). This suggests that the beading seen in the *Prnp^{93N}* mice is related to the overactivation of the NMDA receptor and suggests that excitotoxicity contributes to the spontaneous neurodegeneration the mice experience.

In vitro experiments show that hippocampal neurons are susceptible to excitotoxicity. The NMDA receptor is a heterotetrametric complex made up of GluN1, GluN2A-C, and

GluN3A-B subunits. Synaptic NMDA receptors containing Glun2A are considered neuroprotective, while extrasynaptic NMDA receptors containing Glun2B are considered neurotoxic (Armada-Moreira et al. 2020). The phosphorylation of Glun2B at serine 1303 enhances ion flux, possibly leading to excess Ca^{2+} influx and excitotoxic insult. CaMKII, PKC, and DAPK1 are kinases implicated in phosphorylation of this site (Tavalin and Colbran 2017). Hippocampal samples of the $Prnp^{93N/93N}$ mice at p26 show an increase of phosphorylated CAMKII at Thr286 and phosphorylated GluN2B at ser1303 on western blots (data not shown). This suggests that the $Prnp^{93N}$ hippocampal neurons *in vitro* may experience higher calcium influx and higher ion conductance, leading to increased sensitivity to excitotoxicity and cell death.

Here we found that cortical samples of the $Prnp^{93N/93N}$ mice at p26 show no changes in phosphorylated CAMKII at Thr286 or phosphorylated Glun2B at Ser1303 levels. We suspect that cortical neurons are also experiencing excitotoxicity because the excessive beading in the $Prnp^{93N/93N}$ mice is rescued with an NMDA receptor antagonist. There might not be differences in the cortex because western blot analysis is not sensitive enough to detect cell subtype differences as the hippocampus has a higher population of excitatory neurons than the cortex. Given the present findings, we speculate that the hippocampus is more sensitive to excitotoxic insult than the cortex.

In vivo data support that the neuronal beading seen in the $Prnp^{93N/93N}$ primary neurons is due to NMDA receptor activity. Past studies have shown that PrP[C] interacts with the NMDA receptor (Black et al. 2014). Mice lacking PrP[C] are also more susceptible to excitotoxicity and have more NMDA excitability (Khosravani et al., 2008). We speculate that the added glycan in the N-terminus of the $Prnp^{93N}$ mice alters the interaction between NMDA receptors and PrP[C].

19

Further research is needed to understand the interaction between PrP^C and NMDA receptors in the *Prnp^{93N}* mice. However, this study supports the hypothesis that enhanced signaling through the NMDA receptor contributes to prion-mediated neurodegeneration.

References

Armada-Moreira, Adam, Joana I Gomes, Carolina Campos Pina, Oksana K Savchak, Joana Gonçalves-Ribeiro, Nádia Rei, Sara Pinto, Tatiana Morais, Robertta silva, Filipa Ribeiro, Ana Sebastiao, Vincenzo Crunelli, Sandra Vaz. 2020. "Going the Extra (Synaptic) Mile: Excitotoxicity as the Road Toward Neurodegenerative Diseases." *Frontiers in Cellular Neuroscience* 14: 27.

Biasini, E., U. Unterberger, I. H. Solomon, T. Massignan, A. Senatore, H. Bian, T. Voigtlaender, F. P. Bowman, V. Bonetto, R. Chiesa, J. Luebke, P. Toselli, D. A. Harris. 2013. "A Mutant Prion Protein Sensitizes Neurons to Glutamate-Induced Excitotoxicity." *Journal of Neuroscience* 33 (6): 2408–18. https://doi.org/10.1523/JNEUROSCI.3406-12.2013.

Biasini, Emiliano, Jessie A. Turnbaugh, Ursula Unterberger, and David A. Harris. 2012. "Prion Protein at the Crossroads of Physiology and Disease." *Trends in Neurosciences* 35 (2): 92–103. https://doi.org/10.1016/j.tins.2011.10.002.

Bueler, H, A Aguui, P Autenried, M Ague, and C Weissmann'. n.d. "Mice Devoid of PrP Are Resistant to Scrapie," 9.

Black, Stefanie A. G., Peter K. Stys, Gerald W. Zamponi, and Shigeki Tsutsui. 2014. "Cellular Prion Protein and NMDA Receptor Modulation: Protecting against Excitotoxicity." *Frontiers in Cell and Developmental Biology* 2 (August). https://doi.org/10.3389/fcell.2014.00045.

Brandner, Sebastian, Stefan Isenmann, Alex Raeber, Marek Fischer, Andreas Sailer, Yasushi Kobayashi, Silvia Marino, Charles Weissmann, and Adriano Aguzzi. 1996. "Normal Host Prion Protein Necessary for Scrapie-Induced Neurotoxicity." *Nature* 379 (6563): 339–43. https://doi.org/10.1038/379339a0.

Chen, Cao, and Xiaoping Dong. 2021. "Therapeutic Implications of Prion Diseases." *Biosafety and Health* 3 (2): 92–100. https://doi.org/10.1016/j.bsheal.2020.09.001.

Dametto, Paolo, Asvin K. K. Lakkaraju, Claire Bridel, Lukas Villiger, Tracy O'Connor, Uli S. Herrmann, Pawel Pelczar, Thomas Rulicke, Donal McHugh, Arlind, Adil, Adriano Aguzzi. 2015. "Neurodegeneration and Unfolded-Protein Response in Mice Expressing a Membrane-Tethered Flexible Tail of PrP." Edited by Jiyan Ma. *PLOS ONE* 10 (2): e0117412. https://doi.org/10.1371/journal.pone.0117412.

Dong, Xiao-xia, Yan Wang, and Zheng-hong Qin. 2009. "Molecular Mechanisms of Excitotoxicity and Their Relevance to Pathogenesis of Neurodegenerative Diseases." *Acta Pharmacologica Sinica* 30 (4): 379–87. https://doi.org/10.1038/aps.2009.24.

Donne, D. G., J. H. Viles, D. Groth, I. Mehlhorn, T. L. James, F. E. Cohen, S. B. Prusiner, P. E. Wright, and H. J. Dyson. 1997. "Structure of the Recombinant Full-Length Hamster

Prion Protein PrP(29-231): The N Terminus Is Highly Flexible." *Proceedings of the National Academy of Sciences* 94 (25): 13452–57. https://doi.org/10.1073/pnas.94.25.13452.

Gaudino, Simona, Emma Gangemi, Raffaella Colantonio, Annibale Botto, Emanuela Ruberto, Rosalinda Calandrelli, Matia Martucci, Maria Gabriella Vita, Carlo Mascullo, Alfonso Cerase, Cesare Colosimo. 2017. "Neuroradiology of Human Prion Diseases, Diagnosis and Differential Diagnosis." *La Radiologia Medica* 122 (5): 369–85. https://doi.org/10.1007/s11547-017-0725-y.

Greenwood, Sam M, and Christopher N Connolly. 2007. "Dendritic and Mitochondrial Changes during Glutamate Excitotoxicity," 8.

Hara, Hideyuki, and Suehiro Sakaguchi. 2020. "N-Terminal Regions of Prion Protein: Functions and Roles in Prion Diseases." *International Journal of Molecular Sciences* 21 (17): 6233. https://doi.org/10.3390/ijms21176233.

Khosravani, Houman, Yunfeng Zhang, Shigeki Tsutsui, Shahid Hameed, Christophe Altier, Jawed Hamid, Lina Chen, Michelle Villemaire, Zenobia Ali, Frank Jirik, Gerald Zamponi. 2008. "Prion Protein Attenuates Excitotoxicity by Inhibiting NMDA Receptors." *Journal of Cell Biology* 181 (3): 551–65. https://doi.org/10.1083/jcb.200711002.

Li, Aimin, Heather M Christensen, Leanne R Stewart, Kevin A Roth, Roberto Chiesa, and David A Harris. 2007. "Neonatal Lethality in Transgenic Mice Expressing Prion Protein with a Deletion of Residues 105–125." *The EMBO Journal* 26 (2): 548–58. https://doi.org/10.1038/sj.emboj.7601507.

Lipton, Stuart A. 2004. "Failures and Successes of NMDA Receptor Antagonists: Molecular Basis for the Use of Open-Channel Blockers like Memantine in the Treatment of Acute and Chronic Neurologic Insults" 1 (1): 10.

Mallucci, Giovanna, Andrew Dickinson, Jacqueline Linehan, Peter-Christian Klöhn, Sebastian Brandner, and John Collinge. 2003. "Depleting Neuronal PrP in Prion Infection Prevents Disease and Reverses Spongiosis." *Science* 302 (5646): 871–74. https://doi.org/10.1126/science.1090187.

Mizielinska, Sarah M., Sam M. Greenwood, Hemanth Tummala, and Christopher N. Connolly. 2009. "Rapid Dendritic and Axonal Responses to Neuronal Insults." *Biochemical Society Transactions* 37 (6): 1389–93. https://doi.org/10.1042/BST0371389.

Parsons, Matthew P., and Lynn A. Raymond. 2014. "Extrasynaptic NMDA Receptor Involvement in Central Nervous System Disorders." *Neuron* 82 (2): 279–93. https://doi.org/10.1016/j.neuron.2014.03.030.

Rueden, Curtis T., Johannes Schindelin, Mark C. Hiner, Barry E. DeZonia, Alison E. Walter, Ellen T. Arena, and Kevin W. Eliceiri. 2017. "ImageJ2: ImageJ for the next Generation of Scientific Image Data." *BMC Bioinformatics* 18 (1): 529. https://doi.org/10.1186/s12859-017-1934-z.

Sigurdson, Christina J., Jason C. Bartz, and Markus Glatzel. 2019. "Cellular and Molecular Mechanisms of Prion Disease." *Annual Review of Pathology: Mechanisms of Disease* 14 (1): 497–516. https://doi.org/10.1146/annurev-pathmechdis-012418-013109.

Song, Xianqiang, Morten Ø Jensen, Vishwanath Jogini, Richard A Stein, Chia-Hsueh Lee, Hassane S Mchaourab, David E Shaw, and Eric Gouaux. 2018. "Mechanism of NMDA Receptor Channel Block by MK-801 and Memantine," 32.

Stahl, Neil, Michael Baldwin, Rolf Hecker, Keh-Ming Pan, Alma Burlingame, and Stanley Prusiner. 1992. "Glycosylinositol Phospholipid Anchors of the Scrapie and Cellular Prion Proteins Contain Sialic Acid." *Biochemistry* 31 (21): 5043–53. https://doi.org/10.1021/bi00136a600.

Steele, Andrew D., Susan Lindquist, and Adriano Aguzzi. 2007. "The Prion Protein Knockout Mouse: A Phenotype Under Challenge." *Prion* 1 (2): 83–93. https://doi.org/10.4161/pri.1.2.4346.

Tavalin, Steven J., and Roger J. Colbran. 2017. "CaMKII-Mediated Phosphorylation of GluN2B Regulates Recombinant NMDA Receptor Currents in a Chloride-Dependent Manner." *Molecular and Cellular Neuroscience* 79 (March): 45–52. https://doi.org/10.1016/j.mcn.2016.12.002.

Wang, Chao, Maria A Telpoukhovskaia, Ben A Bahr, Xu Chen, and Li Gan. 2018. "Endo-Lysosomal Dysfunction: A Converging Mechanism in Neurodegenerative Diseases." *Current Opinion in Neurobiology* 48 (February): 52–58. https://doi.org/10.1016/j.conb.2017.09.005.

Westergard, Laura, Heather M. Christensen, and David A. Harris. 2007. "The Cellular Prion Protein (PrPC): Its Physiological Function and Role in Disease." *Biochimica et Biophysica Acta (BBA) - Molecular Basis of Disease* 1772 (6): 629–44. https://doi.org/10.1016/j.bbadis.2007.02.011.

Wu, Bei, Alex J McDonald, Kathleen Markham, Celeste B Rich, Kyle P McHugh, Jörg Tatzelt, David W Colby, Glenn L Millhauser, and David A Harris. 2017. "The N-Terminus of the Prion Protein Is a Toxic Effector Regulated by the C-Terminus." *ELife* 6 (May): e23473. https://doi.org/10.7554/eLife.23473.

Wulf, Marie-Angela, Assunta Senatore, and Adriano Aguzzi. 2017. "The Biological Function of the Cellular Prion Protein: An Update." *BMC Biology* 15 (1): 34. https://doi.org/10.1186/s12915-017-0375-5.

Zahn, R., A. Liu, T. Luhrs, R. Riek, C. von Schroetter, F. Lopez Garcia, M. Billeter, L. Calzolai, G. Wider, and K. Wuthrich. 2000. "NMR Solution Structure of the Human Prion Protein." *Proceedings of the National Academy of Sciences* 97 (1): 145–50. https://doi.org/10.1073/pnas.97.1.145.

Zerr, Inga, and Piero Parchi. 2018. "Sporadic Creutzfeldt–Jakob Disease." In *Handbook of Clinical Neurology*, 153:155–74. Elsevier. https://doi.org/10.1016/B978-0-444-63945-5.00009-X.

Zhang, Yuan, Yanfang Zhao, Lei Zhang, Wanpeng Yu, Yu Wang, and Wenguang Chang. 2019. "Cellular Prion Protein as a Receptor of Toxic Amyloid-B42 Oligomers Is Important for Alzheimer's Disease." *Frontiers in Cellular Neuroscience* 13 (July): 339. https://doi.org/10.3389/fncel.2019.00339.